RESEARCH ARTICLE

WILEY

Reconfiguration of dynamic large-scale brain network functional connectivity in generalized tonic–clonic seizures

Xiaoyan Jia[1] | Yan Xie[2] | Debo Dong[1] | Haonan Pei[1] | Sisi Jiang[1] | Shuai Ma[2] | Yang Huang[1] | Xingxing Zhang[1] | Yuhong Wang[1] | Qiong Zhu[2] | Yanan Zhang[1] | Dezhong Yao[1] | Liang Yu[2] | Cheng Luo[1]

[1]The Clinical Hospital of Chengdu Brain Science Institute, MOE Key Lab for Neuroinformation, Center for Information in Medicine, High-Field Magnetic Resonance Brain Imaging Key Laboratory of Sichuan Province, School of Life Science and Technology, University of Electronic Science and Technology of China, Chengdu, China

[2]Neurology Department, Sichuan Academy of Medical Sciences & Sichuan Provincial People's Hospital, Chengdu, Sichuan, China

Correspondence
Cheng Luo, The Clinical Hospital of Chengdu Brain Science Institute, MOE Key Lab for Neuroinformation, Center for Information in Medicine, High-Field Magnetic Resonance Brain Imaging Key Laboratory of Sichuan Province, School of Life Science and Technology, University of Electronic Science and Technology of China, Chengdu, China.
Email: chengluo@uestc.edu.cn

Liang Yu, Neurology Department, Sichuan Academy of Medical Science & Sichuan Provincial People's Hospital, Chengdu, China.
Email: dyao@uestc.edu.cn

Abstract

An increasing number of studies in patients with generalized tonic–clonic seizures (GTCS) have reported the alteration of functional connectivity (FC) in many brain networks. However, little is known about the underlying temporal variability of FC in large-scale brain functional networks in patients. Recently, dynamic FC could provide novel insight into the physiological mechanisms in the brain. Here, we recruited 63 GTCS and 65 age- and sex-matched healthy controls. Dynamic FC approaches were used to evaluate alterations in the temporal variability of FC in patients at the region- and network-levels. In addition, two kinds of brain templates ($>10^2$ and $> 10^3$ regions) and two kinds of temporal variability FC approaches were adopted to verify the stability of the results. Patients showed increased FC variability in regions of the default mode network (DMN), ventral attention network (VAN) and motor-related areas. The DAN, VAN, and DMN illustrated enhanced FC variability at the within-network level. In addition, increased FC variabilities between networks were found between the DMN and cognition-related networks, including the VAN, dorsal attention network and frontal–parietal network in GTCS. Meanwhile, the alterations in FC variability were relatively consistent across different methods and templates. Therefore, the consistent alteration of FC variability would reflect a dynamic restructuring of the large-scale brain networks in patients with GTCS. Overly frequent information communication among cognition-related networks, especially in the DMN, might play a role in the epileptic activity and/or cognitive dysfunction in patients.

KEYWORDS
epilepsy, functional connectivity, functional magnetic resonance imaging, generalized tonic–clonic seizures, temporal variability

1 | INTRODUCTION

Generalized tonic–clonic seizures (GTCS) is the most common type of seizures in idiopathic generalized epilepsy (IGE) (Nei & Bagla, 2007).

Typical symptoms of GTCS include muscle rigidity of limbs, violent muscle contractions of the entire body and the sudden complete loss of consciousness (Jallon & Latour, 2005; Marini, King, Archer, Newton, & Berkovic, 2003). In addition, cognitive impairments such as attention, memory, and executive dysfunctions were also well documented in patients with GTCS (Hommet, Sauerwein, De Toffol, & Lassonde, 2006; Thompson & Duncan, 2005). However, so far, the underlying mechanism of clinical symptoms in GTCS remains unclear. Therefore, in accompany with the development of neuroimaging methods, understanding the pathophysiological mechanisms of GTCS has become a research priority.

Functional magnetic resonance imaging (fMRI) provides an efficient tool to explore the functional network properties of the human brain (Blatow, Nennig, Durst, Sartor, & Stippich, 2007; Bookheimer, 2002). In recent years, our understanding of how GTCS affects brain networks has been greatly advanced by attempts to map interregional interactions comprising the brain's spontaneous connectivity. Functional interaction between brain networks or regions can be characterized by functional connectivity (FC) (Biswal, Van Kylen, & Hyde, 1997; Gong et al., 2019; Li et al., 2019; Lowe, Dzemidzic, Lurito, Mathews, & Phillips, 2000). Our previous resting state FC study (Jia et al., 2018) and a study by Song et al. (2011) found significantly decreased FC within the default mode network (DMN) in GTCS compared with that in healthy controls (HC), suggesting that abnormal connectivity in DMN might be associated with the impaired consciousness in GTCS. In addition, disrupted interconnections in the DMN, dorsal attention network (DAN), sensorimotor network (SMN), visual network (VN) and auditory network (AN) were observed in IGE, suggesting neural correlates of deficits of self-process and cognitive function in patients (Li et al., 2015; Li et al., 2017; Wang et al., 2011; Zhong et al., 2018). Up to now, many fMRI studies have provided evidence to support the stationary alteration of FC in patients with GTCS during fMRI scanning.

Recently, the temporal variability of FC has attracted increasing attention and has been thought to play an important role in dynamically integrating and coordinating among neural systems in response to stimulation from internal and external environments (Hutchison et al., 2013; Liao et al., 2019; Qin et al., 2019). The previous study suggested that dynamic fluctuations in the brain's large-scale organizational properties might minimize metabolic requirements while maintaining the brain in a responsive state (Zalesky, Fornito, Cocchi, Gollo, & Breakspear, 2014). In dynamic FC analysis in fMRI, overlapping and nonoverlapping sliding window methods have been widely used in several neuropsychiatric disorders such as autism spectrum disorder, attention deficit hyperactivity disorder, schizophrenia and epilepsy (He et al., 2019; Klugah-Brown et al., 2018; Li, Duan, Cui, Chen, & Liao, 2019; Liao et al., 2018; Zhang et al., 2016). In epilepsy, Liao et al found a complex dynamic interaction among functional networks during absence seizures (Liao et al., 2014). Although the study of Liu et al offered preliminary evidence for the changes of the dynamic functional network connectivity metrics in GTCS (Liu et al., 2017), no study regarding GTCS has been performed to comprehensively investigate the temporal variability of FC features from multiple levels such as the region-level and the network-level. A comprehensive investigation of brain dynamic FC allows us to

understand the different dynamic roles of different units in the brain system (Sun et al., 2018). Therefore, the identification of temporal variability of FC features at multiple levels will be crucial to comprehensively understand the pathophysiological mechanism of GTCS.

In the current study, both overlapping and nonoverlapping sliding window dynamic FC approaches were used to reliably and comprehensively evaluate alterations about temporal variability of FC in GTCS based on region-level and network-level. In addition, the previous studies suggested that different scales of brain template might also result in, to some extent, alterations of topological architecture and networks properties (Wang et al., 2009; Xue et al., 2014). To validate the reliability of FC variability on different scales of the brain template, two kinds of brain templates were used in this study, including a hundreds- and a thousand level template. Furthermore, the correlation between altered temporal variability of FC and clinical variables was measured in GTCS. We hypothesized that dynamic FC of large-scale brain network would be reconfigured in GTCS, and DMN might be the highlighted alteration of temporal variability of FC.

2 | MATERIALS AND METHODS

2.1 | Participants

Sixty-three patients with GTCS were recruited in the neurology department, The Affiliated Hospital of the University of the Electronic Science and Technology of China. All patients were diagnosed as IGE with GTCS only by epileptologists (Dr. Yan and Dr. Yu) based on the clinical and seizure semiology information consistent with the International League Against Epilepsy (ILAE) guidelines (Fisher et al., 2017; Scheffer et al., 2017). In detail, patients with GTCS met with the following criteria: (a) typically showed generalized spike–wave activity on scape EEG; (b) showed bilateral and symmetric generalized motor seizures such as tonic, and tonic–clonic seizures with loss of consciousness. Sixty-five HCs were recruited as the age- and gender-matched control group. All subjects are right-handed. Written informed consent was obtained from each individual. The exclusion criteria were as follows: (a) subjects with a history of neurological diseases besides epilepsy, brain structural abnormality, traumatic brain injury or substance abuse; and (b) subjects with magnetic resonance imaging contraindications. This study was approved by the ethical committee of the University of Electronic Science and Technology of China according to the standards of the Declaration of Helsinki.

2.2 | Data acquisition

All subjects underwent MRI scanning in a 3.0 T GE scanner with an eight-channel-phased array head coil (MR750; GE Discovery, Milwaukee, WI). The resting state fMRI data of all subjects were collected using an echo-planar imaging sequence, and the scan parameters were as follows: repetition time (TR) =2000 ms, echo time (TE)=30 ms, matrix=64 ×64, flip angle (FA)= 90 °, field of view (FOV)=24× 24 cm^2, slice thickness =4 mm with a 0.4 mm gap, and 200 volumes were obtained in each run. Axial anatomical T1-weighted data were

acquired using a 3-dimensional fast spoiled gradient echo sequence and with the following scan parameters: TR=6.008 ms, TE =1.984 ms, matrix=256×256, FA =90 °, FOV =25.6 ×25.6 cm^2, slice thickness =1 mm (no gap), 152 axial slices. During scanning, all subjects were instructed to relax, close their eyes, keep awake and not think of anything in particular.

2.3 | Data preprocessing

Preprocessing steps of fMRI data were performed by the Data Processing & Analysis for (Resting-State) Brain Imaging (DPABI, http://rfmri.org/dpabi) software (Yan, Wang, Zuo, & Zang, 2016). The fMRI data were (a) discarded the first five volumes, (b) slice-timing corrected (c) realigned (d) co-registered to 3D anatomic volume, (e) spatially normalized to the Montreal Neurological Institute (MNI) template using estimating nonlinear deformations with determination of 12-parameter affine transformation between individual images and template, and resliced with the voxel size into 3 mm × 3 mm × 3 mm, (f) spatially smoothed by a 6 mm full-width half-maximum Gaussian kernel to improve the signal-to-noise ratio (Worsley & Friston, 1995) like the previous study (Dong et al., 2018), (g) regressed the linear trend signal, 24 head motion parameters (Noonan et al., 1996) and white matter and cerebrospinal fluid signals. Here, the global signal was not considered as a noninteresting regressor, because global signal removal would increase the number of negative FC (Saad et al., 2012) and the previous study suggested the global signal might be beneficial to understand the clinical populations (Hahamy et al., 2014; Yang et al., 2014), (h) band-pass filtered to remove spurious fluctuations in dynamic FC (1/w-0.1 Hz, w is the window duration) (Leonardi & Van De Ville, 2015).

Furthermore, a recent study found that FC is sensitive to head motion signals (Power, Schlaggar, & Petersen, 2015). Therefore, we calculated the framewise displacements (FD) between two successive images:

$$FD = \sqrt{\left(\left(\Delta d_{x_i}\right)^2 + \left(\Delta d_{y_i}\right)^2 + \left(\Delta d_{z_i}\right)^2 + \left(\Delta d_{l_i}\right)^2 + \left(\Delta d_{m_i}\right)^2 + \left(\Delta d_{n_i}\right)^2\right)} \; i = 2, 3, ..., M$$

where M is the length of the time courses (M=195 in our study); x_i, y_i, and z_i are translations; l_i, m_i, and n_i are rotations at the ith time point in the x, y, and z directions; and $\Delta d_{x_i} = x_i - x_{i-1}$, with similar formulas for Δd_{y_i} and Δd_{z_i}. Meanwhile, $\Delta d_{l_i} = 50 \times \pi \times (l_i - l_{i-1})/180$, with similar formulas for Δd_{m_i} and Δd_{n_i}. Additionally, the mean FD was regarded as a covariate in following statistical comparisons (Yan et al., 2013).

2.4 | Temporal variability

Two kinds of brain templates (>10^2 and > 10^3 regions) were adopted. The hundreds level template was adopted connectivity-based parcellation brain atlas (246 regions) created by Fan et al. (2016). Because this template lacks the cerebellum, we added 26 cerebellar regions based on the Anatomical Automatic Labeling atlas (Tzourio-Mazoyer et al., 2002) into hundreds level template. Therefore, the hundreds level template was composed of 272 regions. Similarly, the

thousand level template was also parcellated based on the human cerebral cortex from intrinsic FC by Schaefer and colleagues (Schaefer et al., 2018). In addition, we added subcortical and cerebellar regions from the Craddock-950 atlas (Craddock, James, Holtzheimer, Hu, & Mayberg, 2012) into thousand level template. Thus, the thousand level template consisted of 1,000 cortical regions from the Schaefer-1,000 atlas and 217 subcortical and cerebellar regions from the Craddock-950 atlas. Similar to our previous studies (Dong et al., 2018; Klugah-Brown et al., 2018), the temporal variability of FC was evaluated, and the same calculation pipeline was carried out in the two-scale brain templates.

2.5 | Temporal variability of region-level FC architecture

The average BOLD time series were extracted for each region. To evaluate the temporal variability of the FC architecture associated with a brain region, the time series of all regions (N) were segmented into n nonoverlapping sliding windows each with length l (Figure 1a). Within the ith time window, an N × N Pearson correlation matrix was obtained to represent the FC of the whole brain (F_i). The whole-brain FC architecture of region k at the time window i is an N-dimensional vector, which is described as $F_{i, k}$ and the variability of region k is defined as:

$$V_k = 1 - \overline{corrcoef\left(F_{i,k}, F_{j,k}\right)}, i, j = 1, 2, 3, \cdots, n, i \neq j$$

V_k was calculated in different window lengths (l = 10, 11, 12, ..., 20 volumes) to avoid the arbitrary choice of time window length. And the final variability of the region was obtained by taking the average value of all different window lengths (Zhang et al., 2016).

In addition, the previous study indicated that the resting state dynamic FC analysis is most strongly influenced by the offset between two successive sliding windows (Shakil, Lee, & Keilholz, 2016), the overlapping sliding window method was also used in this study. In consideration of the controversy how to define the window length, we selected a range of window lengths (20, 21, 22, ..., 50 TR) (Hutchison, Womelsdorf, Gati, Everling, & Menon, 2013). And the typical window step between sliding windows adopted in previous studies ranges from one TR to 50% of the window length (Chang, Liu, Chen, Liu, & Duyn, 2013; Klugah-Brown et al., 2018; Liu et al., 2017). The main calculation about window step in this study was set as 40% of window length. In addition, to avoid the arbitrary choice of window step, 30 and 50% of the window length were also explored to validate the reliability of the results. The calculation of FC variability was also the same as the nonoverlapping sliding window, the calculation chart was demonstrated in Figure 1.

2.5.1 | Temporal variability of network-level FC architecture

The variability of FC architecture between two networks or within a specific network was calculated based on the N regions of the brain
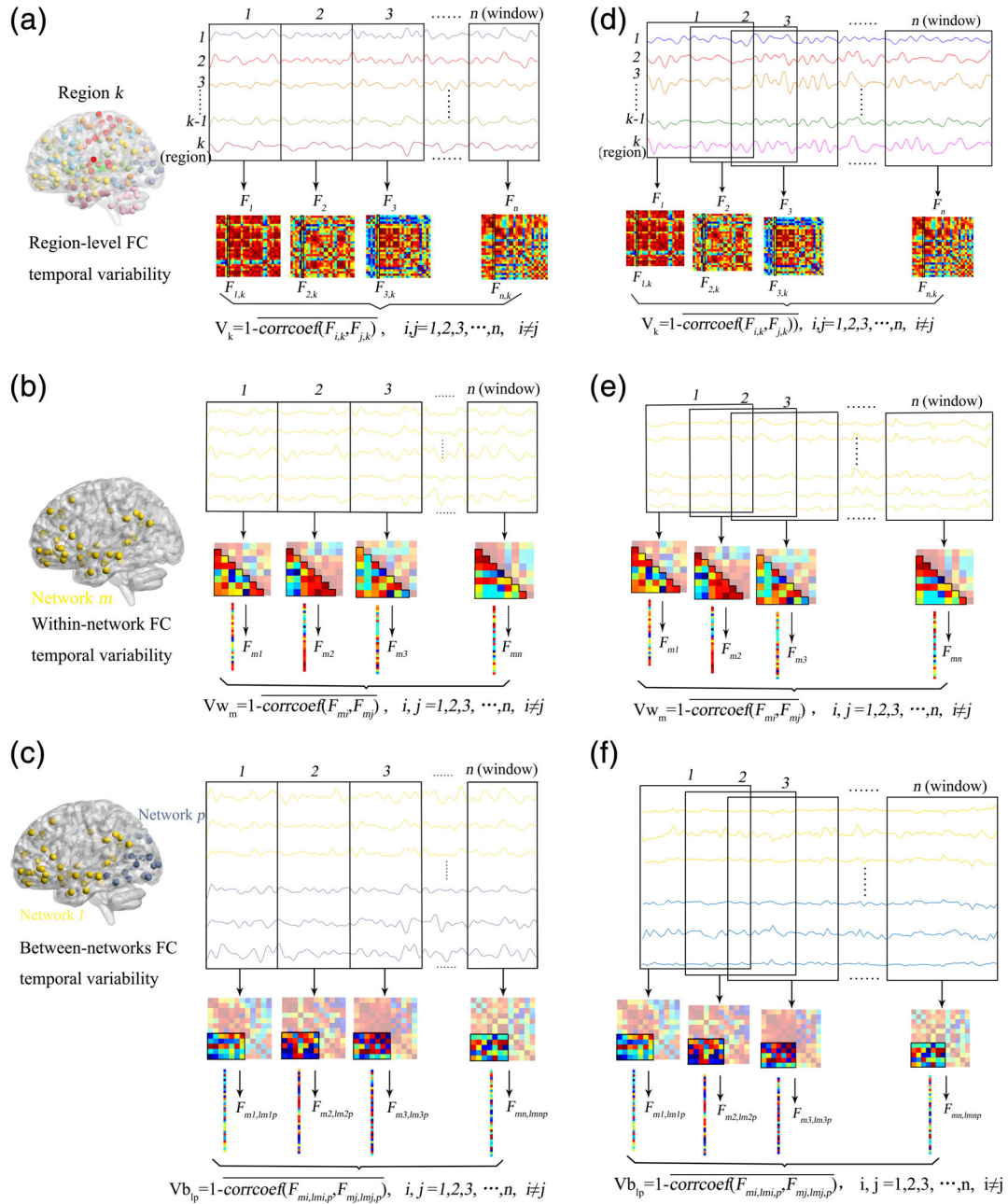
FIGURE 1 Chart of calculation for nonoverlapping sliding window (a,b,c) and overlapping sliding window (d,e,f). (a) Region-level FC variability for nonoverlapping sliding window. (b) Within-network FC variability for nonoverlapping sliding window. (c) Between-networks FC variability for nonoverlapping sliding window. (d) Region-level FC variability for overlapping sliding window. (e) Within-network FC variability for overlapping sliding window. (f) Between-networks FC variability for overlapping sliding window

template. Since cerebellum and subcortical nuclei are important regions in epilepsy, cerebellum regions were included in the cerebellar network (CereN), and subcortical nuclei regions were included in subcortical nuclei (SubN). The remaining regions were divided into seven brain networks, including VN, SMN, DAN, VAN, limbic network (LN), frontal–parietal network (FPN) and DMN based on previous studies that segmented whole brain networks (Yeo et al., 2011). The variability of functional architecture between or within the brain network was calculated by similar procedures used in regional brain variability above (Sun et al., 2018). For a given brain network m, all FCs within

this network in the time window i was reshaped as a one-dimensional vector, F_{mi} (Figure 1b). For all FCs, between-network l and network p in the window i were denoted as one-dimensional vectors, $F_{mi, lmip}$ (Figure 1c). The within-network temporal variability of network m is defined as follows:

$$Vw_m = 1 - \overline{corrcoef\left(F_{mi}, F_{mj}\right)} \ i,j = 1,2,3,\cdots,n, i \neq j$$

and the between-network temporal variability of network l and network p is defined as:

$$Vb_{1p} = 1 - \overline{corrcoef\left(F_{mi,lmi,p}, F_{mj,lmj,p}\right)}\, i,j = 1,2,3,\cdots,n, i \neq j$$

The temporal variability within-network characterizes whether the FCs within a particular network is changing synchronously across different time windows. Similarly, between-network temporal variability depicts the pattern of FC between two different networks across different time windows.

The overlapping sliding window method was also carried out at the network-level. The window length and step were the same as the calculation of region-level FC variability by the overlapping sliding window method, and the calculation of FC variability at the network-level was the same as the nonoverlapping sliding window method mentioned before.

2.5.2 | Validation analysis

To evaluate the discreteness of the correlation value among different windows, we further calculated the coefficient variation (CV) of the four styles of FC variability mentioned above. For example, the CV of region k on the region-level for a given window length was defined as follows:

$$CV_k = \frac{std\left(corrcoef\left(F_{i,k}, F_{j,k}\right)\right)}{mean\left(corrcoef\left(F_{i,k}, F_{j,k}\right)\right)}, i,j = 1,2,3,\cdots,n, i \neq j$$

The final CV of region k was obtained by taking the average value of all the different window lengths. A similar calculation was carried out on the network-level.

2.6 | Statistical analysis

To evaluate the variability differences between patients and HCs, a two-sample t-test was carried out on the individual variability of regions, and the within and between brain network variability; moreover, the mean FD was regressed out as a covariate, with a significance set at $p < .05$ (false discovery rate corrected, FDR).

In addition, we calculated the partial correlations between the years of disease duration and the significantly altered variability of FC in the GTCS group, the age of onset was regressed out as a covariate to control the influence of brain development caused by seizures early in life (Holmes, 2005), with a significance set at $p < .01$.

3 | RESULTS

Six patients and five HCs were excluded because of head motion scans exceeding 2 mm and/or 2°. Twelve patients and two HCs were discarded with framewise displacements (FD) of successive images more than 0.5 mm. Therefore, 45 GTCS and 58 HCs were included in the final analysis. There was no significant difference in the mean FD between patients and HCs (patients, mean=0.043, SD=0.022; HCs, mean=0.038, SD=0.018; p=.147, t=1.463). And there was no significant difference in the age (patients, mean = 23.02, SD = 11.88; HCs,

mean = 24.09, SD = 11.13; p = 0.64, two-sample t-test) and gender (p = .47, χ^2 test). The detailed clinical information about all patients is shown in Supplementary Table 1.

The alterations in FC variability were relatively stable across different methods and templates. We highlighted the same alterations across different methods and templates in supporting materials.

3.1 | Temporal variability based on the nonoverlapping sliding window method (hundreds level)

Compared with the variabilities in HCs, significantly increased temporal variability at the region-level was found in the insula, cerebellum, precentral gyrus, basal ganglia, precuneus, cingulum gyrus, and in some regions of the frontal–parietal cortex in GTCS (Figure 2a, Supplementary Table 2). Figure 3 showed the alteration within-network, however, temporal variability of within-network with hundreds level templates was not observed.

Compared with the variabilities in HCs, significantly increased temporal variabilities of FC between-networks were observed between the DMN and VAN in GTCS (Figure 4a, Table 1).

3.2 | Temporal variability based on the overlapping sliding window method (hundreds level)

Compared with the variabilities in HCs, patients with GTCS showed significantly increased temporal variability at the region-level in the insula, cerebellum, precentral gyrus, precuneus, cingulum gyrus, and some regions of frontal–parietal cortex (Figure 2b, Supplementary Table 3), which was similar to the results of the nonoverlapping window method in the hundreds level template. In addition, temporal variabilities within-networks was also not observed here.
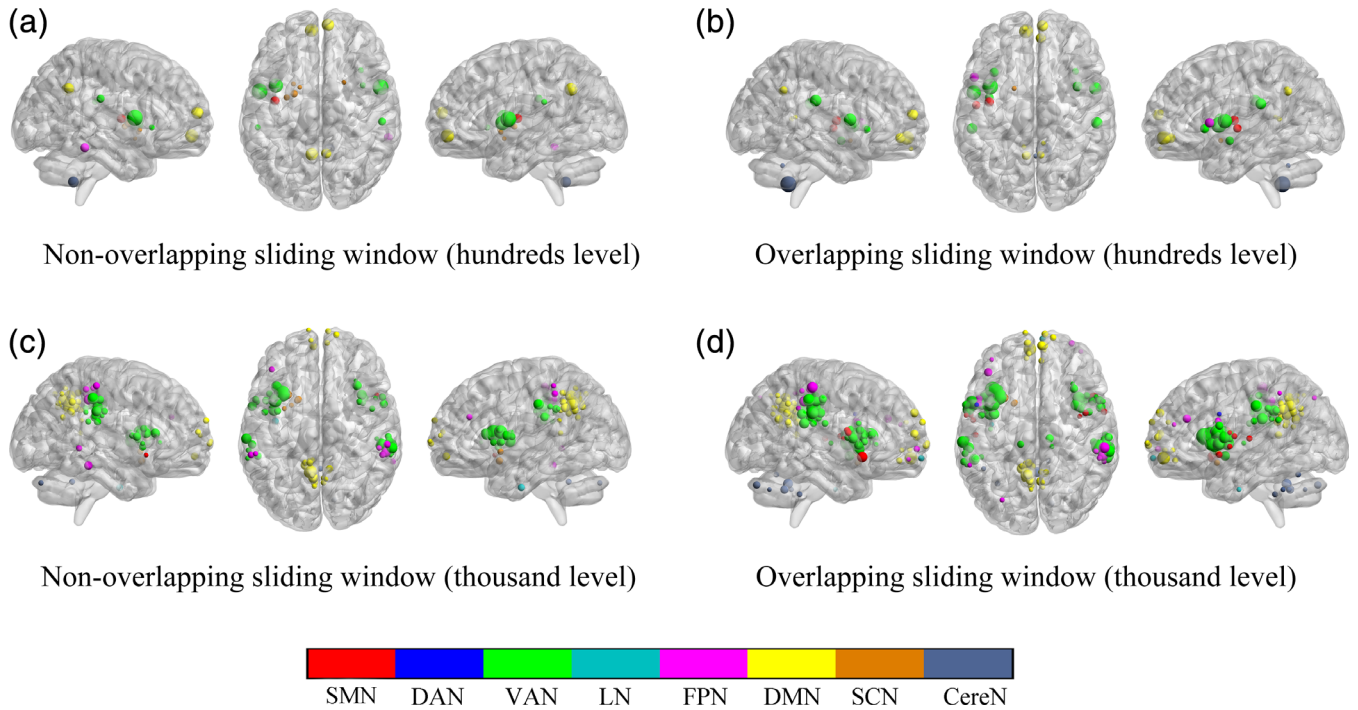
Compared with the variabilities in HCs, significantly increased temporal variabilities of FC between-networks were observed between the DMN and DAN, the DMN and VAN, and the DMN and FPN in the GTCS (Figure 4b, Table 1).

3.3 | Temporal variability based on the nonoverlapping sliding window method (thousand level)

Compared with the variabilities in HCs, significantly increased temporal variability at the region-level was observed in the frontal–parietal related regions, insula, precuneus, pre- and postcentral gyrus, basal ganglia, cerebellum and cingulate gyrus to the whole brain in the GTCS (Figure 2c, Supplementary Table 4).

Compared with the variabilities in HCs, patients with GTCS demonstrated significantly increased temporal variabilities within-networks in the VAN, DAN and DMN (Figure 3a, Table 1). In addition, significantly increased temporal variabilities of FC between-networks were observed between the DMN and VAN, and the DMN and FPN in the GTCS (Figure 4c, Table 1).

(a) Non-overlapping sliding window (hundreds level)

(b) Overlapping sliding window (hundreds level)

(c) Non-overlapping sliding window (thousand level)

(d) Overlapping sliding window (thousand level)

SMN   DAN   VAN   LN   FPN   DMN   SCN   CereN

FIGURE 2 Group differences in FC temporal variability of region-level (FDR corrected, $p < .05$). CereN, cerebellar network; DAN, dorsal attention network; DMN, default mode network; LN, limbic network; FPN, frontal–parietal network; SCN, subcortical nuclei network; SMN, sensorimotor network; VAN, ventral attention network

(a) Non-overlapping sliding window (thousand level)

(b) Overlapping sliding window (thousand level)
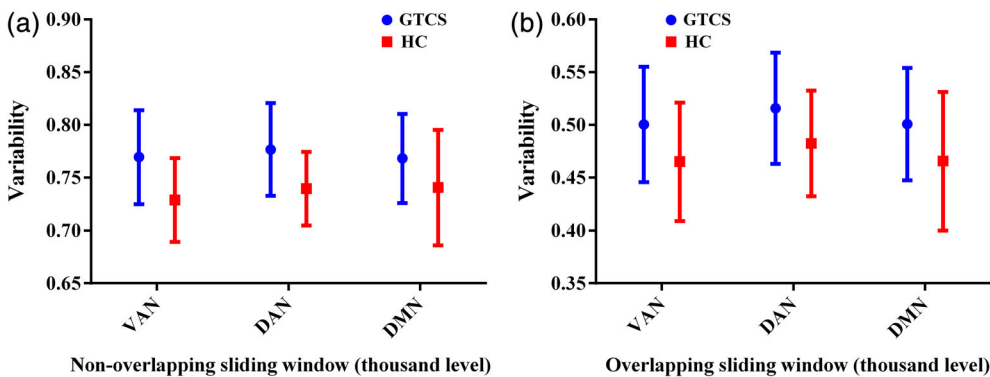
FIGURE 3 Group differences in FC temporal variability of within-network level (FDR corrected, $p < .05$). DAN, dorsal attention network; DMN, default mode network; VAN, ventral attention network

3.4 | Temporal variability based on the overlapping sliding window method (thousand level)

The results of temporal variability at the region-level were similar to the results based on the nonoverlapping window method at the thousand level template, that is, significantly increased temporal variability was observed in the frontal–parietal association regions, insula, pre- and postcentral gyrus, precuneus, cerebellum, cingulate gyrus, and few regions of the basal ganglia to the whole brain in GTCS (Figure 2d, Supplementary Table 5).

Similar to the results of the nonoverlapping window method at the thousand level template, significantly increased temporal variability of the within-network was still found in the VAN, DAN and DMN (Figure 3b and Table 1). In addition, significantly increased temporal variabilities of FC were observed between the DMN and VAN, the

DMN and FPN, the DAN and VAN, and the DMN and DAN in the GTCS (Figure 4d and Table 1).

In addition, when the step between sliding windows was set as 30% and 50% of window length, the results of temporal variability at the region-level network-level were similar to that with the step set as 40% of window length. Correspondingly, those supplementary results of temporal variability at the region-level, within-network level, and between-networks level were demonstrated in Supplementary Figure 1, Supplementary Figure 2, and Supplementary Figure 3.

3.5 | CV of correlation value

Compared with the variabilities in HCs, significantly increased CV in the region-level with the hundreds level template was mainly observed in the precentral gyrus, insula, basal ganglia, cerebellum, and

FIGURE 4 Group differences in FC temporal variability of between-networks level (FDR corrected, $p < .05$). DAN, dorsal attention network; DMN, default mode network; FPN, frontal–parietal network; VAN, ventral attention network
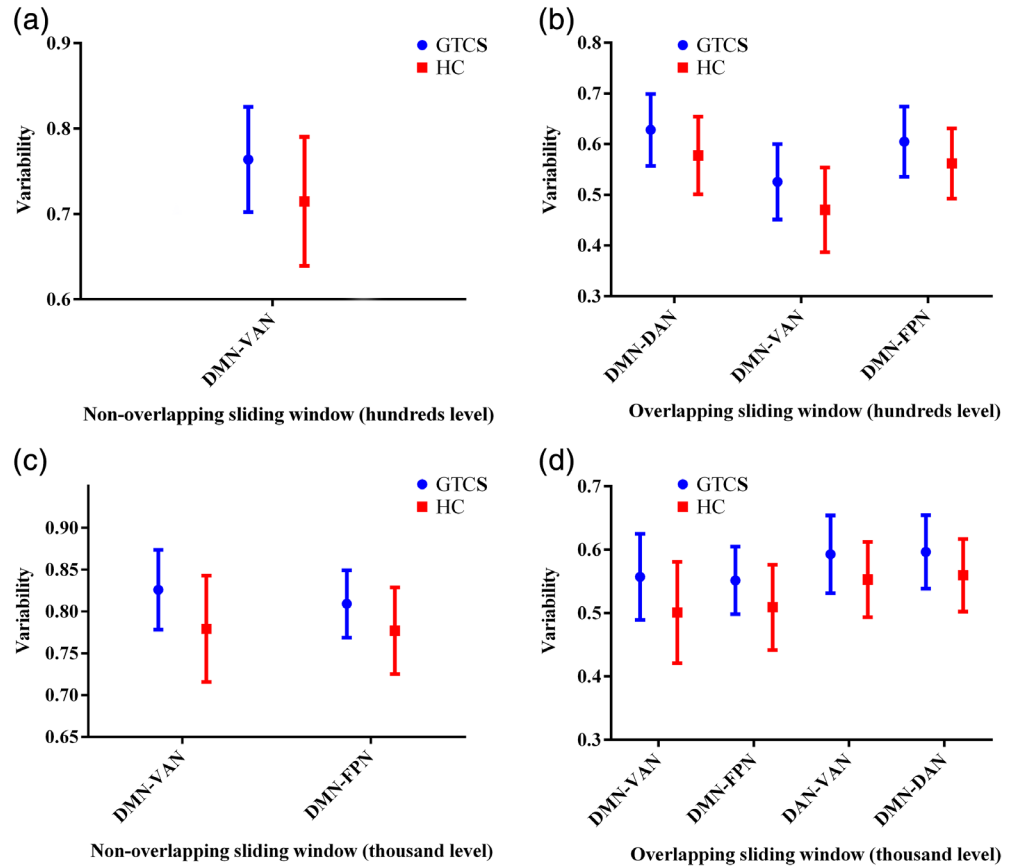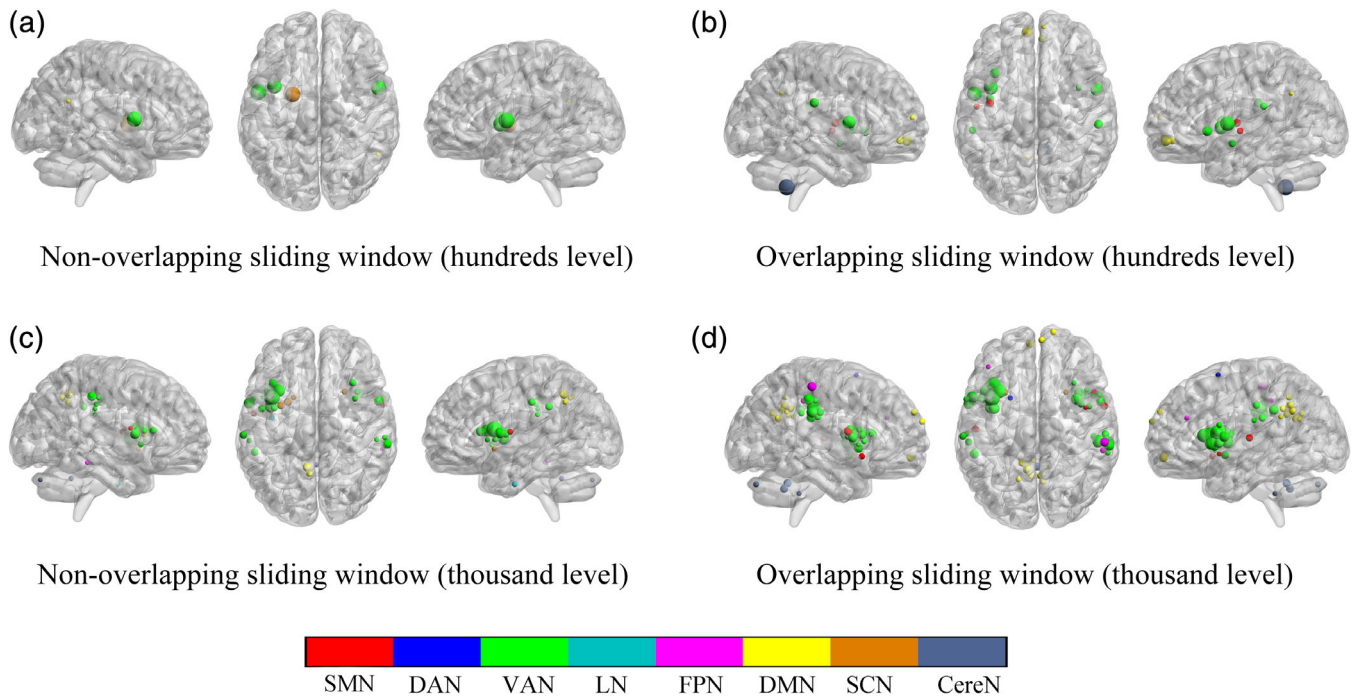

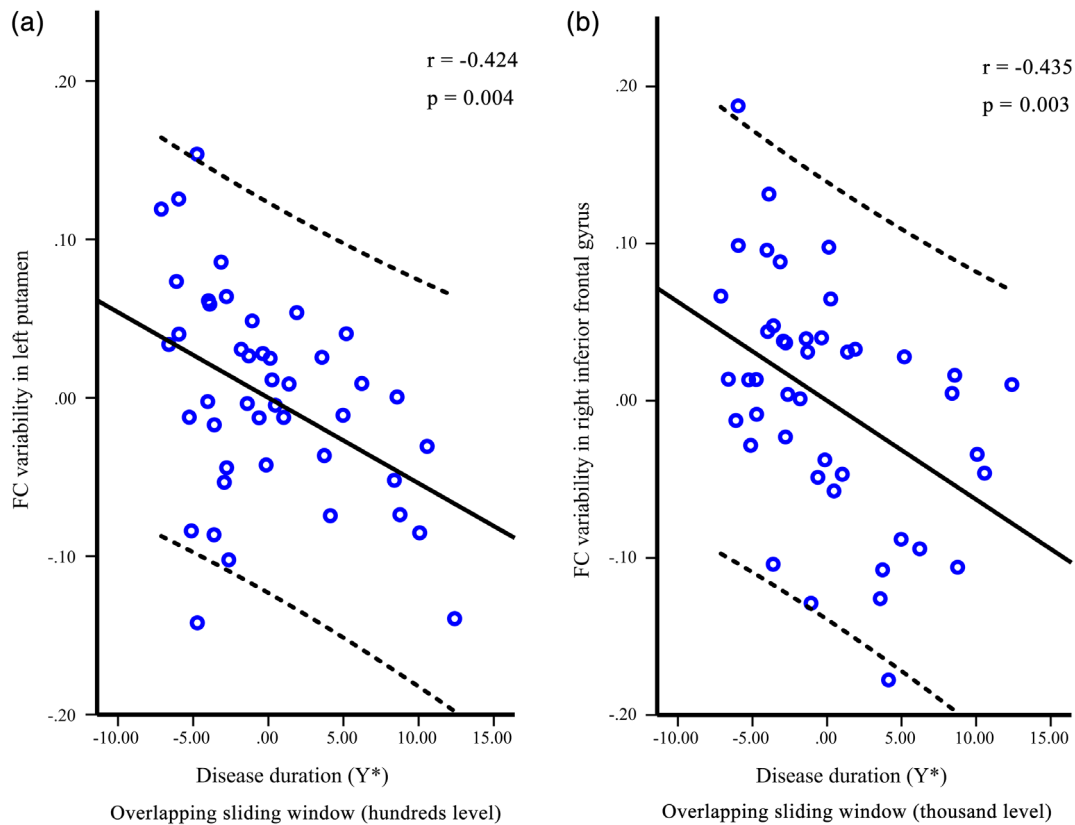**TABLE 1** Group differences of FC variability within or between network(s)

Type of temporal variability	Patients		HCs		
	Mean	SD	Mean	SD	p value
Nonoverlapping sliding window (hundreds level)					
DMN-VAN	0.764	0.062	0.713	0.076	.035
Overlapping sliding window (hundreds level)					
DMN-DAN	0.628	0.071	0.578	0.077	.033
DMN-VAN	0.526	0.075	0.470	0.083	.033
DMN-FPN	0.605	0.069	0.562	0.069	.043
Nonoverlapping sliding window (thousand level)					
VAN	0.770	0.044	0.729	0.040	.017
DAN	0.777	0.044	0.740	0.035	.020
DMN	0.768	0.042	0.741	0.055	.035
DMN-VAN	0.826	0.048	0.779	0.063	.008
DMN-FPN	0.809	0.040	0.777	0.052	.029
Overlapping sliding window (thousand level)					
VAN	0.500	0.055	0.465	0.056	.020
DAN	0.516	0.053	0.482	0.050	.020
DMN	0.501	0.053	0.466	0.066	.034
DMN-VAN	0.557	0.068	0.501	0.080	.024
DMN-FPN	0.552	0.053	0.509	0.067	.032
DAN-VAN	0.593	0.061	0.553	0.060	.023
DMN-DAN	0.597	0.058	0.559	0.057	.032

Note: FDR corrected $p<.05$.
Abbreviations: DAN, dorsal attention network; DMN, default mode network; FPN, frontal–parietal network; SD, standard deviation; VAN, ventral attention network.

(a)

Non-overlapping sliding window (hundreds level)

(b)

Overlapping sliding window (hundreds level)

(c)

Non-overlapping sliding window (thousand level)

(d)

Overlapping sliding window (thousand level)

SMN   DAN   VAN   LN   FPN   DMN   SCN   CereN

FIGURE 5 Group differences in CV of region-level FC architecture (FDR corrected, $p < .05$). SMN: sensorimotor network. DAN: dorsal attention network. VAN: ventral attention network. LN: limbic network. FPN: frontal–parietal network. DMN: default mode network. SCN: subcortical nuclei network. CereN: cerebellar network

(a)

r = -0.424
p = 0.004

FC variability in left putamen

Disease duration (Y*)

Overlapping sliding window (hundreds level)

(b)

r = -0.435
p = 0.003

FC variability in right inferior frontal gyrus

Disease duration (Y*)

Overlapping sliding window (thousand level)

FIGURE 6 Correlation between FC variability and years of disease duration. Y* represents the disease duration (years) after controlling for the effect of the age of onset. One outlier was removed (> mean ± 2*SD) for the correlation calculation

inferior partial gyrus (Figure 5a,b, Supplementary Table 6). A significantly increased CV in the region-level with the thousand level template was observed in insula, frontal–parietal association regions, pre- postcentral gyrus, precuneus, cerebellum, and basal ganglia (Figure 5c,d, Supplementary Table 6).

Compared with HCs, significant changes in GTCS at the network-level were only found when using an overlapping sliding window at the thousand level template. Significantly increased CV in the within-network level was found in the DAN and VAN (Supplementary Figure 4 A, Supplementary Table 7), and significantly increased CV in the between-networks level was found between the DMN and VAN, the DMN and DAN, and the DAN and VAN in the GTCS (Supplementary Figure 4 B, Supplementary Table 7).

3.6 | Correlation analysis between FC variability and clinical variables

After controlling for the effect of the age of onset, significant correlations between FC variability and clinical variables were only revealed between FC variability at the region-level and the years of disease duration. In detail, temporal variability in the left putamen on the hundreds level template was significantly related with illness duration in patients (Figure 6a). The significant correlation was observed in the right inferior frontal gyrus temporal variability with the overlapping sliding window in the thousand level template (Figure 6b).

4 | DISCUSSION

In the present study, two types of FC temporal variability were used to comprehensively investigate the reconfiguration of large-scale brain network dynamic FC analysis in IGE with GTCS only for the first time. Importantly, the observation is relatively consistent across different brain region templates and different dynamic FC methods. Increased FC temporal variability at the region-level was observed in the insula, cerebellum, pre- and postcentral gyrus, precuneus, cingulum gyrus, basal ganglia and some regions of the frontal–parietal related cortex in GTCS. Increased temporal variabilities of within-network FC architecture were found in the VAN, DAN, and DMN. And this alteration was only observed in the thousand level brain template analysis. Meanwhile, increased temporal variabilities of between-network FC architecture were observed between the DMN and VAN, the DMN and DAN, the DMN and FPN, and DAN and VAN across the two types of brain templates with overlapping sliding window dynamic FC methods in the GTCS. Furthermore, increased variation coefficients of FC variability were also observed in the GTCS. In addition, there were significant correlations between FC variability at the region-level and disease duration (years) in GTCS. This study provides novel insight into the pathophysiological mechanisms of GTCS.

To our knowledge, this is the first study to explore the dynamic FC in GTCS in a large-scale brain network. Significantly increased FC temporal variability in the region-level of GTCS was revealed in regions of the VAN and DMN such as the insula, precuneus, cingulum

and frontal lobe. Interestingly, significantly increased FC temporal variability of the VAN and DMN was also observed in the within-network level. Previous study suggested that the insula plays a crucial role in integrating disparate functional systems such as affects, sensory-motor, and general cognition; Offering an interface between action, feelings, and cognition (Chang, Yarkoni, Khaw, & Sanfey, 2013). Similar to the importance of the role of the insula in the human brain, emerging studies have shown that the functional hubs of the brain are mostly located in DMN (Tomasi & Volkow, 2011; van den Heuvel & Sporns, 2013). The DMN is engaged in the consciousness of episodic memory and/or self-awareness (Raichle et al., 2001; T. Yang et al., 2013). Thus, we speculated that overly frequent information communication in regions of the VAN and DMN might be associated with the impairment of automatic bottom-up salience detection after chronic epilepsy discharge and attention lapses and memory deficits in GTCS.

In addition, it is worth noting that the increased FC temporal variability in the DMN was not only found at the region-level but also revealed at the between-networks level, which further suggested that the DMN plays a crucial role in GTCS. The temporal variability of FC between the DMN and VAN, the DMN and FPN, the DMN and DAN, and the VAN and DAN were significantly increased in the GTCS. Normally, the DMN is activated in the resting state and reflects spontaneous thought processes, such as meditation and introspection (Brewer et al., 2011; Raichle et al., 2001); the DAN and VAN are activated in the task state and are mainly involved in externally oriented mental processes to maintain and reorient attention (Christoff, Irving, Fox, Spreng, & Andrews-Hanna, 2016). In addition, the FPN is thought to be responsible for cognitive control functions such as working memory, attentional selection and error monitoring (Vincent, Kahn, Snyder, Raichle, & Buckner, 2008). Meanwhile, the DMN is also considered a key network, especially when considering its ability to integrate information from cognition and primary function networks (Raichle et al., 2001). The interaction between the DMN and task-positive networks (the DAN, VAN, and FPN) reflects the switch between the intrinsic and extrinsic focus of attention (Weissman, Roberts, Visscher, & Woldorff, 2006; Whitfield-Gabrieli & Ford, 2012). Study indicated the relatively low variability of the DMN in normal physiologic conditions because of its strong FC within the network during the resting state (Zhang et al., 2016). In line with the study of Liu et al (Liu et al., 2017), abnormal FC temporal variability between the DMN and task-positive networks was found in GTCS. Taken together, the increased variability between the DMN and task-positive networks might lead to a functional confusion of task-negative and task-positive networks and disadvantages in maintaining cognitive function, which might be related to the dysfunction of cognition in GTCS.

Besides, significantly increased temporal variability of FC at the region-level was found in the basal ganglia, cerebellum, pre- and postcentral gyrus in this study. Previous study demonstrated that the basal ganglia is involved in motor selection, preparation, and execution (Emmanuel et al., 2004). In addition, the basal ganglia is also widely considered in the implication of modulating of the spike and wave discharges in epilepsy (Norden & Blumenfeld, 2002). A previous study demonstrated that controlling the output from the cerebellar cortex

could effectively interrupt seizures (Kros, Eelkman Rooda, De Zeeuw, & Hoebeek, 2015). Damage of the cerebellum would lead to a disorder of movement equilibrium and motor learning (Fine, Ionita, & Lohr, 2002). The pre- and postcentral gyrus was also found to be increased in the activation of epilepsy (Jiang et al., 2016; Klugah-Brown et al., 2019). Therefore, the abnormal FC temporal variability of the basal ganglia, cerebellum, and pre- post central might be associated with motor dysfunction during seizures in GTCS. In addition, the FC variability in putamen was correlated with the illness duration. Because many patients in this study was treated by antiepileptic drugs (AEDs), we suspected that the lower FC variability in patients with longer illness duration might reflect the effect of treatment with AEDs. Hermans and colleagues found significantly increased FC in patients with IGE after the withdrawal of AEDs, which suggested that AEDs inhibit the propagation of seizures through reducing the synchronous firing of neuronal ensembles (Hermans et al., 2015). It is also possible that the compensatory mechanism in patients with long duration might contribute to the altered FC variability in these regions. Besides, the thalamus is considered as a key pathophysiological node in IGE (Jiang et al., 2018). However, we did not find any significant results in thalamus on region-level or network-level. We suspect that the selected templates are more focus on the cerebral cortex and the number of nodes in the thalamus is limited, which does not allow us to investigate the thalamus FC variability.

Furthermore, the alterations of FC variability within the network were only revealed in the thousand level template. The findings suggested that different scales of brain templates reflected different insights for alterations of FC variability in GTCS. In addition, to highlight the benefits of adopting the dynamic FC, we also calculated the static FC using a similar procedure, as we mentioned in Supplementary materials. We found significantly increased FC of precuneus, cingulum and superior frontal gyrus, as well as significantly decreased FC of cerebellum and basal ganglia in patients. But no significant result was found in network level. This result was similar with the previous studies (T. Yang et al., 2013; Zhong et al., 2018), and might suggest that the static FC reflects one side of specific alteration in patients with GTCS. Meanwhile, the findings strengthened the necessity of FC temporal variability in company with static FC analysis to explore the dysfunction in IGE.

While we believe this study offers comprehensive and reliable findings by using two levels of FC temporal variability with two levels of brain templates and two kinds of methods of dynamic FC, there are still several limitations that need to be addressed in future studies. First, most patients recruited in this study were medicated. Previous study suggested that taking antiepileptic drugs can affect normal neuronal and cognitive function (Loring & Meador, 2004). Therefore, future studies should consider the influence of antiepileptic drugs in FC temporal variability. Second, electroencephalography combined with fMRI was not used in this study since it is difficult for participants to continue to not move their head during scanning. Electroencephalography combined with MRI would help evaluate the relationship between interictal epileptiform discharge during scanning and FC temporal variability. Third, previous studies indicated that head movements can affect the estimate of FC (Power et al., 2015; Satterthwaite et al., 2013). Even if we tried our best to avoid this problem, including discarding data with high and frequent head motion, regressing 24 motion parameters, regressing out the mean FD during statistical analysis, the effect of head motion could not be entirely ruled out. Besides, well-matched FD subgroups analysis was carried out, which was showed in Supplementary materials, and we found the main results still remained (Supplementary Figure 5–7). Finally, it should be noted that, there is no data on the cognitive assessments in the present study, and direct relationship cannot be established between our results and cognition data. Although we suspected that the changes of FC temporal variability in the cognition-related network in patients with GTCS were related to the cognitive dysfunction of GTCS, it will be a very meaningful topic to establish the relationship between dynamic FC changes and cognition in future research.

5 | CONCLUSION

In summary, patients with GTCS demonstrated the reliable abnormality of FC temporal variability in cognition related functional networks, especially in the DMN, suggesting overly frequent information communication among them, which might implicate epileptic activity and cognitive deficits in patients. In addition, increased FC temporal variability in motor-related regions might be associated with motor dysfunction in GTCS. These findings provide novel neuroimaging evidence for the hypothesis of reconfiguration of the dynamic large-scale brain network in GTCS. Overall, the dynamic FC analysis sheds light on understanding the pathophysiology mechanisms of GTCS.

DISCLOSURE

None of authors has any conflict of interest to disclose. We confirm that we have read the Journal's position on issues involved in ethical publication and affirm that this report is consistent with those guidelines.

Data Availability Statement

The data that support the findings of this study are available on request from the corresponding author. The data are not publicly available due to privacy or ethical restrictions.

ORCID

Xiaoyan Jia https://orcid.org/0000-0002-3730-6877
Cheng Luo https://orcid.org/0000-0003-0524-5886

REFERENCES

Biswal, B. B., Van Kylen, J., & Hyde, J. S. (1997). Simultaneous assessment of flow and BOLD signals in resting-state functional connectivity maps. *NMR in Biomedicine*, *10*(4–5), 165–170.

Blatow, M., Nennig, E., Durst, A., Sartor, K., & Stippich, C. (2007). fMRI reflects functional connectivity of human somatosensory cortex. *NeuroImage*, *37*(3), 927–936. https://doi.org/10.1016/j.neuroimage.2007.05.038

Bookheimer, S. (2002). Functional MRI of language: New approaches to understanding the cortical organization of semantic processing. *Annual Review of Neuroscience*, *25*, 151–188. https://doi.org/10.1146/annurev.neuro.25.112701.142946

Brewer, J. A., Worhunsky, P. D., Gray, J. R., Tang, Y. Y., Weber, J., & Kober, H. (2011). Meditation experience is associated with differences in default mode network activity and connectivity. *Proceedings of the National Academy of Sciences of the United States of America*, *108*(50), 20254–20259. https://doi.org/10.1073/pnas.1112029108

Chang, C., Liu, Z., Chen, M. C., Liu, X., & Duyn, J. H. (2013). EEG correlates of time-varying BOLD functional connectivity. *NeuroImage*, *72*, 227–236. https://doi.org/10.1016/j.neuroimage.2013.01.049

Chang, L. J., Yarkoni, T., Khaw, M. W., & Sanfey, A. G. (2013). Decoding the role of the insula in human cognition: Functional parcellation and large-scale reverse inference. *Cerebral Cortex*, *23*(3), 739–749. https://doi.org/10.1093/cercor/bhs065

Christoff, K., Irving, Z. C., Fox, K. C. R., Spreng, R. N., & Andrews-Hanna, J. R. (2016). Mind-wandering as spontaneous thought: A dynamic framework. *Nature Reviews Neuroscience*, *17*(11), 718–731. https://doi.org/10.1038/nrn.2016.113

Craddock, R. C., James, G. A., Holtzheimer, P. E., Hu, X. P. P., & Mayberg, H. S. (2012). A whole brain fMRI atlas generated via spatially constrained spectral clustering. *Human Brain Mapping*, *33*(8), 1914–1928. https://doi.org/10.1002/hbm.21333

Dong, D., Duan, M., Wang, Y., Zhang, X., Jia, X., Li, Y., ... Luo, C. (2018). Reconfiguration of dynamic functional connectivity in sensory and perceptual system in schizophrenia. *Cerebral Cortex*, *29*, 3577–3589. https://doi.org/10.1093/cercor/bhy232

Emmanuel, G., Jean-Baptiste, P., Jean-Baptiste, P., Léon, T., Pierre-Fran? Ois, V. D. M., Richard, L., ... Stéphane, L. (2004). Distinct striatal regions support movement selection, preparation and execution. *Neuroreport*, *15*(15), 2327–2331.

Fan, L. Z., Li, H., Zhuo, J. J., Zhang, Y., Wang, J. J., Chen, L. F., ... Jiang, T. Z. (2016). The human Brainnetome atlas: A new brain atlas based on connectional architecture. *Cerebral Cortex*, *26*(8), 3508–3526. https://doi.org/10.1093/cercor/bhw157

Fine, E. J., Ionita, C. C., & Lohr, L. (2002). The history of the development of the cerebellar examination. *Seminars in Neurology*, *22*(4), 375–384. https://doi.org/10.1055/s-2002-36759

Fisher, R. S., Cross, J. H., French, J. A., Higurashi, N., Hirsch, E., Jansen, F. E., ... Roulet, P. E. (2017). Operational classification of seizure types by the international league against epilepsy: Position paper of the ILAE Commission for Classification and Terminology. *Epilepsia*, *58*(4), 522–530.

Gong, J., Luo, C., Li, X., Jiang, S., Khundrakpam, B. S., Duan, M., ... Yao, D. (2019). Evaluation of functional connectivity in subdivisions of the thalamus in schizophrenia. *The British Journal of Psychiatry*, *214*(5), 288–296. https://doi.org/10.1192/bjp.2018.299

Hahamy, A., Calhoun, V., Pearlson, G., Harel, M., Stern, N., Attar, F., ... Salomon, R. (2014). Save the global: Global signal connectivity as a tool for studying clinical populations with functional magnetic resonance imaging. *Brain Connectivity*, *4*(6), 395–403. https://doi.org/10.1089/brain.2014.0244

He, H., Luo, C., Luo, Y., Duan, M., Yi, Q., Biswal, B. B., & Yao, D. (2019). Reduction in gray matter of cerebellum in schizophrenia and its influence on static and dynamic connectivity. *Human Brain Mapping*, *40*(2), 517–528. https://doi.org/10.1002/hbm.24391

Hermans, K., Ossenblok, P., van Houdt, P., Geerts, L., Verdaasdonk, R., Boon, P., ... de Munck, J. C. (2015). Network analysis of EEG related functional MRI changes due to medication withdrawal in focal epilepsy. *Neuroimage Clinical*, *8*, 560–571. https://doi.org/10.1016/j.nicl.2015.06.002

Holmes, G. L. (2005). Effects of seizures on brain development: Lessons from the laboratory. *Pediatric Neurology*, *33*(1), 1–11. https://doi.org/10.1016/j.pediatrneurol.2004.12.003

Hommet, C., Sauerwein, H. C., De Toffol, B., & Lassonde, M. (2006). Idiopathic epileptic syndromes and cognition. *Neuroscience and Biobehavioral Reviews*, *30*(1), 85–96. https://doi.org/10.1016/j.neubiorev.2005.06.004

Hutchison, R. M., Womelsdorf, T., Allen, E. A., Bandettini, P. A., Calhoun, V. D., Corbetta, M., ... Chang, C. (2013). Dynamic functional connectivity: Promise, issues, and interpretations. *NeuroImage*, *80*, 360–378. https://doi.org/10.1016/j.neuroimage.2013.05.079

Hutchison, R. M., Womelsdorf, T., Gati, J. S., Everling, S., & Menon, R. S. (2013). Resting-state networks show dynamic functional connectivity in awake humans and anesthetized macaques. *Human Brain Mapping*, *34*(9), 2154–2177. https://doi.org/10.1002/hbm.22058

Jallon, P., & Latour, P. (2005). Epidemiology of idiopathic generalized epilepsies. *Epilepsia*, *46*(Suppl 9), 10–14. https://doi.org/10.1111/j.1528-1167.2005.00309.x

Jia, X., Ma, S., Jiang, S., Sun, H., Dong, D., Chang, X., ... Luo, C. (2018). Disrupted coupling between the spontaneous fluctuation and functional connectivity in idiopathic generalized epilepsy. *Frontiers in Neurology*, *9*, 838. https://doi.org/10.3389/fneur.2018.00838

Jiang, S., Luo, C., Gong, J., Peng, R., Ma, S., Tan, S., ... Yao, D. (2018). Aberrant Thalamocortical connectivity in juvenile myoclonic epilepsy. *International Journal of Neural Systems*, *28*(1), 1750034. https://doi.org/10.1142/S0129065717500344

Jiang, S., Luo, C., Liu, Z., Hou, C., Wang, P., Dong, L., ... Yao, D. (2016). Altered local spontaneous brain activity in juvenile myoclonic epilepsy: A preliminary resting-state fMRI study. *Neural Plasticity*, *2016*, 3547203–3547207. https://doi.org/10.1155/2016/3547203

Klugah-Brown, B., Luo, C., He, H., Jiang, S., Armah, G. K., Wu, Y., ... Yao, D. (2018). Altered dynamic functional network connectivity in frontal lobe epilepsy. *Brain Topography*, *32*, 394–404. https://doi.org/10.1007/s10548-018-0678-z

Klugah-Brown, B., Luo, C., Peng, R., He, H., Li, J. F., Dong, L., & Yao, D. Z. (2019). Altered structural and causal connectivity in frontal lobe epilepsy. *BMC Neurology*, *19*, 70. https://doi.org/10.1186/s12883-019-1300-z

Kros, L., Eelkman Rooda, O. H. J., De Zeeuw, C. I., & Hoebeek, F. E. (2015). Controlling cerebellar output to treat refractory epilepsy. *Trends in Neurosciences*, *38*(12), 787–799. https://doi.org/10.1016/j.tins.2015.10.002

Leonardi, N., & Van De Ville, D. (2015). On spurious and real fluctuations of dynamic functional connectivity during rest. *NeuroImage*, *104*, 430–436. https://doi.org/10.1016/j.neuroimage.2014.09.007

Li, H., Cao, W., Zhang, X., Sun, B., Jiang, S., Li, J., ... Luo, C. (2019). BOLD-fMRI reveals the association between renal oxygenation and functional connectivity in the aging brain. *NeuroImage*, *186*, 510–517. https://doi.org/10.1016/j.neuroimage.2018.11.030

Li, J., Duan, X., Cui, Q., Chen, H., & Liao, W. (2019). More than just statics: Temporal dynamics of intrinsic brain activity predicts the suicidal ideation in depressed patients. *Psychological Medicine*, *49*(5), 852–860. https://doi.org/10.1017/S0033291718001502

Li, Q., Cao, W., Liao, X., Chen, Z., Yang, T., Gong, Q., ... Yao, D. (2015). Altered resting state functional network connectivity in children absence epilepsy. *Journal of the Neurological Sciences*, *354*(1–2), 79–85. https://doi.org/10.1016/j.jns.2015.04.054

Li, R., Yu, Y., Liao, W., Zhang, Z., Lu, G., & Chen, H. (2017). Disrupted architecture of large-scale brain functional connectivity networks in patients with generalized tonic–clonic seizure. *Applied Informatics*, *4* (1), 15.

Liao, W., Fan, Y.-S., Yang, S., Li, J., Duan, X., Cui, Q., & Chen, H. (2018). Preservation effect: Cigarette smoking acts on the dynamic of influences among unifying neuropsychiatric triple networks in schizophrenia. *Schizophrenia Bulletin*. https://doi.org/10.1093/schbul/sby184

Liao, W., Li, J., Ji, G. J., Wu, G. R., Long, Z., Xu, Q., ... Chen, H. (2019). Endless fluctuations: Temporal dynamics of the amplitude of low frequency fluctuations. *IEEE Transactions on Medical Imaging*. https://doi.org/10.1109/TMI.2019.2904555

Liao, W., Zhang, Z., Mantini, D., Xu, Q., Ji, G. J., Zhang, H., ... Lu, G. (2014). Dynamical intrinsic functional architecture of the brain during absence seizures. *Brain Structure & Function*, *219*(6), 2001–2015. https://doi.org/10.1007/s00429-013-0619-2

Liu, F., Wang, Y. F., Li, M. L., Wang, W. Q., Li, R., Zhang, Z. Q., ... Chen, H. F. (2017). Dynamic functional network connectivity in idiopathic generalized epilepsy with generalized tonic-clonic seizure. *Human Brain Mapping*, *38*(2), 957–973. https://doi.org/10.1002/hbm.23430

Loring, D. W., & Meador, K. J. (2004). Cognitive side effects of antiepileptic drugs in children. *Neurology*, *62*(6), 872–877.

Lowe, M. J., Dzemidzic, M., Lurito, J. T., Mathews, V. P., & Phillips, M. D. (2000). Correlations in low-frequency BOLD fluctuations reflect cortico-cortical connections. *NeuroImage*, *12*(5), 582–587. https://doi.org/10.1006/nimg.2000.0654

Marini, C., King, M. A., Archer, J. S., Newton, M. R., & Berkovic, S. F. (2003). Idiopathic generalised epilepsy of adult onset: Clinical syndromes and genetics. *Journal of Neurology, Neurosurgery, and Psychiatry*, *74*(2), 192–196.

Nei, M., & Bagla, R. (2007). Seizure-related injury and death. *Current Neurology and Neuroscience Reports*, *7*(4), 335–341.

Noonan, F. P., Webber, L. J., De Fabo, E. C., Hoffman, H. A., Bendich, A., & Mathews-Roth, M. (1996). Dietary beta-carotene and ultraviolet-induced immunosuppression. *Clinical and Experimental Immunology*, *103*(1), 54–60.

Norden, A. D., & Blumenfeld, H. (2002). The role of subcortical structures in human epilepsy. *Epilepsy & Behavior*, *3*(3), 219–231.

Power, J. D., Schlaggar, B. L., & Petersen, S. E. (2015). Recent progress and outstanding issues in motion correction in resting state fMRI. *NeuroImage*, *105*, 536–551. https://doi.org/10.1016/j.neuroimage.2014.10.044

Qin, Y., Jiang, S., Zhang, Q., Dong, L., Jia, X., He, H., ... Yao, D. (2019). BOLD-fMRI activity informed by network variation of scalp EEG in juvenile myoclonic epilepsy. *Neuroimage Clinical*, *22*, 101759. https://doi.org/10.1016/j.nicl.2019.101759

Raichle, M. E., MacLeod, A. M., Snyder, A. Z., Powers, W. J., Gusnard, D. A., & Shulman, G. L. (2001). A default mode of brain function. *Proceedings of the National Academy of Sciences of the United States of America*, *98*(2), 676–682. https://doi.org/10.1073/pnas.98.2.676

Saad, Z. S., Gotts, S. J., Murphy, K., Chen, G., Jo, H. J., Martin, A., & Cox, R. W. (2012). Trouble at rest: How correlation patterns and group differences become distorted after global signal regression. *Brain Connectivity*, *2*(1), 25–32. https://doi.org/10.1089/brain.2012.0080

Satterthwaite, T. D., Elliott, M. A., Gerraty, R. T., Ruparel, K., Loughead, J., Calkins, M. E., ... Wolf, D. H. (2013). An improved framework for confound regression and filtering for control of motion artifact in the preprocessing of resting-state functional connectivity data. *NeuroImage*, *64*, 240–256. https://doi.org/10.1016/j.neuroimage.2012.08.052

Schaefer, A., Kong, R., Gordon, E. M., Laumann, T. O., Zuo, X. N., Holmes, A. J., ... Thomas, B. T. (2018). Local-global Parcellation of the human cerebral cortex from intrinsic functional connectivity MRI. *Cerebral Cortex*, *28*(9), 3095–3114. https://doi.org/10.1093/cercor/bhx179

Scheffer, I. E., Berkovic, S., Capovilla, G., Connolly, M. B., French, J., Guilhoto, L., ... Moshé, S. L. (2017). ILAE classification of the epilepsies: Position paper of the ILAE Commission for Classification and Terminology. *Epilepsia*, *58*(4), 512–521.

Shakil, S., Lee, C. H., & Keilholz, S. D. (2016). Evaluation of sliding window correlation performance for characterizing dynamic functional connectivity and brain states. *NeuroImage*, *133*, 111–128. https://doi.org/10.1016/j.neuroimage.2016.02.074

Song, M., Du, H. J., Wu, N., Hou, B., Wu, G. C., Wang, J. A., ... Jiang, T. Z. (2011). Impaired resting-state functional integrations within default mode network of generalized tonic-Clonic seizures epilepsy. *Plos One*, *6*(2), e17294. https://doi.org/10.1371/journal.pone.0017294

Sun, J., Liu, Z., Rolls, E. T., Chen, Q., Yao, Y., Yang, W., ... Qiu, J. (2018). Verbal creativity correlates with the temporal variability of brain networks during the resting state. *Cerebral Cortex*, *29*, 1047–1058. https://doi.org/10.1093/cercor/bhy010

Thompson, P. J., & Duncan, J. S. (2005). Cognitive decline in severe intractable epilepsy. *Epilepsia*, *46*(11), 1780–1787. https://doi.org/10.1111/j.1528-1167.2005.00279.x

Tomasi, D., & Volkow, N. D. (2011). Association between functional connectivity hubs and brain networks. *Cerebral Cortex*, *21*(9), 2003–2013. https://doi.org/10.1093/cercor/bhq268

Tzourio-Mazoyer, N., Landeau, B., Papathanassiou, D., Crivello, F., Etard, O., Delcroix, N., ... Joliot, M. (2002). Automated anatomical labeling of activations in SPM using a macroscopic anatomical parcellation of the MNI MRI single-subject brain. *NeuroImage*, *15*(1), 273–289. https://doi.org/10.1006/nimg.2001.0978

van den Heuvel, M. P., & Sporns, O. (2013). Network hubs in the human brain. *Trends in Cognitive Sciences*, *17*(12), 683–696. https://doi.org/10.1016/j.tics.2013.09.012

Vincent, J. L., Kahn, I., Snyder, A. Z., Raichle, M. E., & Buckner, R. L. (2008). Evidence for a frontoparietal control system revealed by intrinsic functional connectivity. *Journal of Neurophysiology*, *100*(6), 3328–3342. https://doi.org/10.1152/jn.90355.2008

Wang, J., Wang, L., Zang, Y., Yang, H., Tang, H., Gong, Q., ... He, Y. (2009). Parcellation-dependent small-world brain functional networks: A resting-state fMRI study. *Human Brain Mapping*, *30*(5), 1511–1523. https://doi.org/10.1002/hbm.20623

Wang, Z. G., Lu, G. M., Zhang, Z. Q., Zhong, Y. A., Jiao, Q., Zhang, Z. J., ... Liu, Y. J. (2011). Altered resting state networks in epileptic patients with generalized tonic-clonic seizures. *Brain Research*, *1374*, 134–141. https://doi.org/10.1016/j.brainres.2010.12.034

Weissman, D. H., Roberts, K. C., Visscher, K. M., & Woldorff, M. G. (2006). The neural bases of momentary lapses in attention. *Nature Neuroscience*, *9*(7), 971–978. https://doi.org/10.1038/nn1727

Whitfield-Gabrieli, S., & Ford, J. M. (2012). Default mode network activity and connectivity in psychopathology. *Annual Review of Clinical Psychology*, *8*, 49–76. https://doi.org/10.1146/annurev-clinpsy-032511-143049

Worsley, K. J., & Friston, K. J. (1995). Analysis of fMRI time-series revisited--again. *NeuroImage*, *2*(3), 173–181. https://doi.org/10.1006/nimg.1995.1023

Xue, K., Luo, C., Zhang, D., Yang, T., Li, J., Gong, D., ... Yao, D. (2014). Diffusion tensor tractography reveals disrupted structural connectivity in childhood absence epilepsy. *Epilepsy Research*, *108*(1), 125–138. https://doi.org/10.1016/j.eplepsyres.2013.10.002

Yan, C. G., Cheung, B., Kelly, C., Colcombe, S., Craddock, R. C., Di Martino, A., ... Milham, M. P. (2013). A comprehensive assessment of regional variation in the impact of head micromovements on functional connectomics. *NeuroImage*, *76*, 183–201. https://doi.org/10.1016/j.neuroimage.2013.03.004

Yan, C. G., Wang, X. D., Zuo, X. N., & Zang, Y. F. (2016). DPABI: Data Processing & Analysis for (resting-state) brain imaging.

Neuroinformatics, *14*(3), 339–351. https://doi.org/10.1007/s12021-016-9299-4

Yang, G. J., Murray, J. D., Repovs, G., Cole, M. W., Savic, A., Glasser, M. F., … Anticevic, A. (2014). Altered global brain signal in schizophrenia. *Proceedings of the National Academy of Sciences of the United States of America*, *111*(20), 7438–7443. https://doi.org/10.1073/pnas.1405289111

Yang, T., Luo, C., Li, Q., Guo, Z., Liu, L., Gong, Q., … Zhou, D. (2013). Altered resting-state connectivity during interictal generalized spike-wave discharges in drug-naive childhood absence epilepsy. *Human Brain Mapping*, *34*(8), 1761–1767. https://doi.org/10.1002/hbm.22025

Yeo, B. T., Krienen, F. M., Sepulcre, J., Sabuncu, M. R., Lashkari, D., Hollinshead, M., … Buckner, R. L. (2011). The organization of the human cerebral cortex estimated by intrinsic functional connectivity. *Journal of Neurophysiology*, *106*(3), 1125–1165. https://doi.org/10.1152/jn.00338.2011

Zalesky, A., Fornito, A., Cocchi, L., Gollo, L. L., & Breakspear, M. (2014). Time-resolved resting-state brain networks. *Proceedings of the National Academy of Sciences of the United States of America*, *111*(28), 10341–10346. https://doi.org/10.1073/pnas.1400181111

Zhang, J., Cheng, W., Liu, Z. W., Zhang, K., Lei, X., Yao, Y., … Feng, J. F. (2016). Neural, electrophysiological and anatomical basis of brain-network variability and its characteristic changes in mental disorders. *Brain*, *139*, 2307–2321. https://doi.org/10.1093/brain/aww143

Zhong, C. Q., Liu, R., Luo, C., Jiang, S. S., Dong, L., Peng, R., … Wang, P. (2018). Altered structural and functional connectivity of juvenile myoclonic epilepsy: An fMRI study. *Neural Plasticity*, *2018*, 7392187. https://doi.org/10.1155/2018/7392187

SUPPORTING INFORMATION

Additional supporting information may be found online in the Supporting Information section at the end of this article.